Cross-Coupling Reactions Hot Paper

How to cite: *Angew. Chem. Int. Ed.* **2022,** *61,* e202211433
International Edition: doi.org/10.1002/anie.202211433
German Edition: doi.org/10.1002/ange.202211433

Intraligand Charge Transfer Enables Visible-Light-Mediated Nickel-Catalyzed Cross-Coupling Reactions**

Cristian Cavedon[+], Sebastian Gisbertz[+], Susanne Reischauer, Sarah Vogl, Eric Sperlich, John H. Burke, Rachel F. Wallick, Stefanie Schrottke, Wei-Hsin Hsu, Lucia Anghileri, Yannik Pfeifer, Noah Richter, Christian Teutloff, Henrike Müller-Werkmeister, Dario Cambié, Peter H. Seeberger, Josh Vura-Weis, Renske M. van der Veen, Arne Thomas,* and Bartholomäus Pieber**

Abstract: We demonstrate that several visible-light-mediated carbon–heteroatom cross-coupling reactions can be carried out using a photoactive Ni^{II} precatalyst that forms in situ from a nickel salt and a bipyridine ligand decorated with two carbazole groups ($Ni(Czbpy)Cl_2$). The activation of this precatalyst towards cross-coupling reactions follows a hitherto undisclosed mechanism that is different from previously reported light-responsive nickel complexes that undergo metal-to-ligand charge transfer. Theoretical and spectroscopic investigations revealed that irradiation of $Ni(Czbpy)Cl_2$ with visible light causes an initial intraligand charge transfer event that triggers productive catalysis. Ligand polymerization affords a porous, recyclable organic polymer for heterogeneous nickel catalysis of cross-coupling reactions. The heterogeneous catalyst shows stable performance in a packed-bed flow reactor during a week of continuous operation.

Introduction

Transition-metal-catalyzed cross-coupling reactions are key to the synthesis of fine chemicals.[1,2] Nickel catalysts are an abundant alternative to palladium complexes, particularly by combining nickel- and photocatalysis in a dual catalytic approach (metallaphotocatalysis).[3–8] This catalytic strategy enables the use of bench-stable, commercially available Ni^{II} salts, and bipyridine ligands that form the nickel catalyst in situ. Photocatalysts for metallaphotocatalyzed cross-coupling reactions range from ruthenium and iridium polypyridyl complexes and organic dyes to heterogeneous semiconductors, including polymers.[6] The initial mechanistic hypothesis for dual photo/nickel-catalyzed carbon–heteroatom cross-coupling reactions suggested that energy or electron transfer between the photocatalyst and a thermodynamically stable Ni^{II} intermediate triggers reductive elimination of the desired product.[6,9] Recent evidence suggests that these reactions proceed through Ni^{I}/Ni^{III} cycles (Figure 1).[10–12] These findings imply that the role of the photocatalyst (PC) is in the generation of a catalytically active Ni^{I} species through a single-electron reduction of the Ni^{II} precatalyst and Ni^{II} resting states (Figure 1a). This is supported by a protocol that uses sub-stoichiometric

[*] C. Cavedon,[+] S. Gisbertz,[+] S. Reischauer, W.-H. Hsu, L. Anghileri, N. Richter, D. Cambié, P. H. Seeberger, B. Pieber
Department of Biomolecular Systems,
Max-Planck-Institute of Colloids and Interfaces
Am Mühlenberg 1, 14476 Potsdam (Germany)
E-mail: bartholomaeus.pieber@mpikg.mpg.de

C. Cavedon,[+] S. Gisbertz,[+] S. Reischauer, L. Anghileri, P. H. Seeberger
Department of Chemistry and Biochemistry,
Freie Universität Berlin
Arnimallee 22, 14195 Berlin (Germany)

S. Vogl, A. Thomas
Department of Chemistry, Functional Materials,
Technische Universität Berlin
Hardenbergstraße 40, 10623 Berlin (Germany)
E-mail: arne.thomas@tu-berlin.de

E. Sperlich, Y. Pfeifer, H. Müller-Werkmeister
Institute of Chemistry, University of Potsdam
Karl-Liebknecht-Strasse 24–25, 14476 Potsdam (Germany)

J. H. Burke, R. F. Wallick, J. Vura-Weis, R. M. van der Veen
Department of Chemistry, University of Illinois Urbana-Champaign
Urbana, Illinois 61801 (USA)

S. Schrottke, C. Teutloff
Department of Physics, Freie Universität Berlin
Arnimallee 22, 14195 Berlin (Germany)

R. M. van der Veen
Helmholtz Zentrum Berlin für Materialien und Energie GmbH
Hahn-Meitner-Platz 1, 14109 Berlin (Germany)
E-mail: renske.vanderveen@helmholtz-berlin.de

[+] These authors contributed equally to this work.

[**] A previous version of this manuscript has been deposited on a preprint server (https://doi.org/10.26434/chemrxiv-2021-kt2wr).

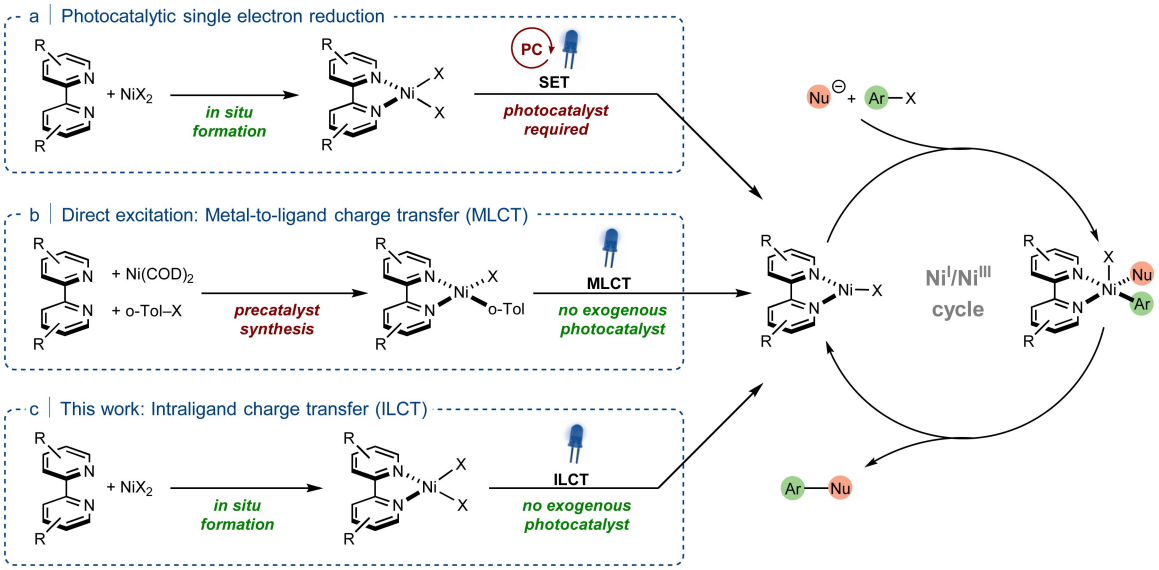

Figure 1. Strategies for visible-light-mediated nickel-catalyzed carbon–heteroatom cross-couplings. a) Dual photo/nickel-catalysis uses in situ-formed nickel precatalyst and an exogenous photocatalyst. b) Ni^{II}(dtbbpy) aryl halide complexes can be activated via MLCT. c) In situ-formed nickel precatalysts can be activated via ILCT (this work).

amounts of zinc in place of a photocatalyst and light for C–N and C–O cross-couplings.[13]

Doyle and co-workers showed that these key Ni^{I} species can be accessed without photocatalysts or additives by illuminating Ni^{II}(dtbbpy) aryl halide complexes (dtbbpy = 4,4′-di-*tert*-butyl-2,2′-bipyridyl), which are synthesized from $Ni(COD)_2$ (COD = 1,5-cyclooctadiene) or nickel phosphine complexes (Figure 1b).[14,15] Here, excitation generates a metal-to-ligand charge transfer (MLCT) state that either decays to a triplet metal-centered d-d state,[14] or a ligand-to-metal charge transfer (LMCT) state.[16,17] The weakened bonds in these latter states were reported to result in homolysis of the Ni^{II}-aryl bond to generate the key Ni^{I} catalyst, thereby initiating cross-coupling catalysis.[14,15] The scope of this photocatalyst-free strategy was studied for C–O and C–N cross-coupling reactions using ultraviolet (UV, 390 nm) irradiation.[18,19]

Inspired by Doyle's elegant strategy, we wondered whether modification of the bipyridine ligand could access a catalytically active Ni^{I} species through intraligand charge transfer (ILCT; Figure 1c). We hypothesized that a ligand-centered excited state would decay into a labile metal-centered d-d state undergoing bond homolysis to initiate cross-coupling catalysis. Here, we demonstrate that this can be achieved by decorating a bipyridine ligand with two carbazole units. The resulting complex enables visible-light-mediated C–O, C–S, and C–N cross-coupling of nucleophiles with aryl halides. Heterogeneous catalysis was realized by polymerizing the ligand. The resulting conjugated microporous polymer coordinates nickel and serves as a recyclable heterogeneous catalyst for light-mediated carbon–heteroatom cross-coupling reactions. The robust catalyst showed stable performance during one week of operation in continuous flow mode using a packed-bed reactor.

Results and Discussion

Our underlying strategy was to equip the bipyridine ligand with a structural motif that allows intraligand charge transfer upon light excitation in the visible. Inspired by organic donor–acceptor fluorophores, such as 1,2,3,5-tetrakis-(carbazol-9-yl)-4,6-dicyanobenzene (4CzIPN),[20,21] we decided to decorate a bipyridine motif with two carbazole units as electron donor moieties via a copper-catalyzed Ullmann coupling (Figure 2a).[22] The resulting 5,5′-dicarbazolyl-2,2′-bipyridyl (Czbpy) forms the desired Ni(Czbpy)Cl_2 complex upon mixing with $NiCl_2$·glyme. A comparison of the electrochemical properties of this complex with Ni(dtbbpy)Cl_2, which is commonly used in metallaphotocatalytic cross-coupling reactions, shows that Ni(Czbpy)Cl_2 is easier to reduce (Figure 2b). Furthermore, the cyclic voltammogram of Ni(Czbpy)Cl_2 shows two additional reduction waves that are tentatively assigned as ligand reductions.

The UV/Visible spectrum of the unbound Czbpy ligand shows a broad and strong absorption band in the UV region (λ_{max} = 343 nm; Figure 2c). Complexation with $NiCl_2$·glyme gave a red-shift of this band with an absorption onset in the visible region of the electromagnetic spectrum (onset ~450 nm, λ_{max} = 386 nm). The structure of this absorption band, its extinction coefficient, and the fluorescence lifetime are similar for the complex and the unbound ligand, indicating that they share the same origin (see the Supporting Information for details). To determine the nature of the electronic transitions, time-dependent density functional theory (TD-DFT) calculations were performed (see the Supporting Information for details). The transition that makes up the 386 nm band in the experimental spectrum of the complex is of predominantly ILCT character, involving the transfer of electron density from the carbazole groups to the bipyridine moiety (the highest occupied molecular

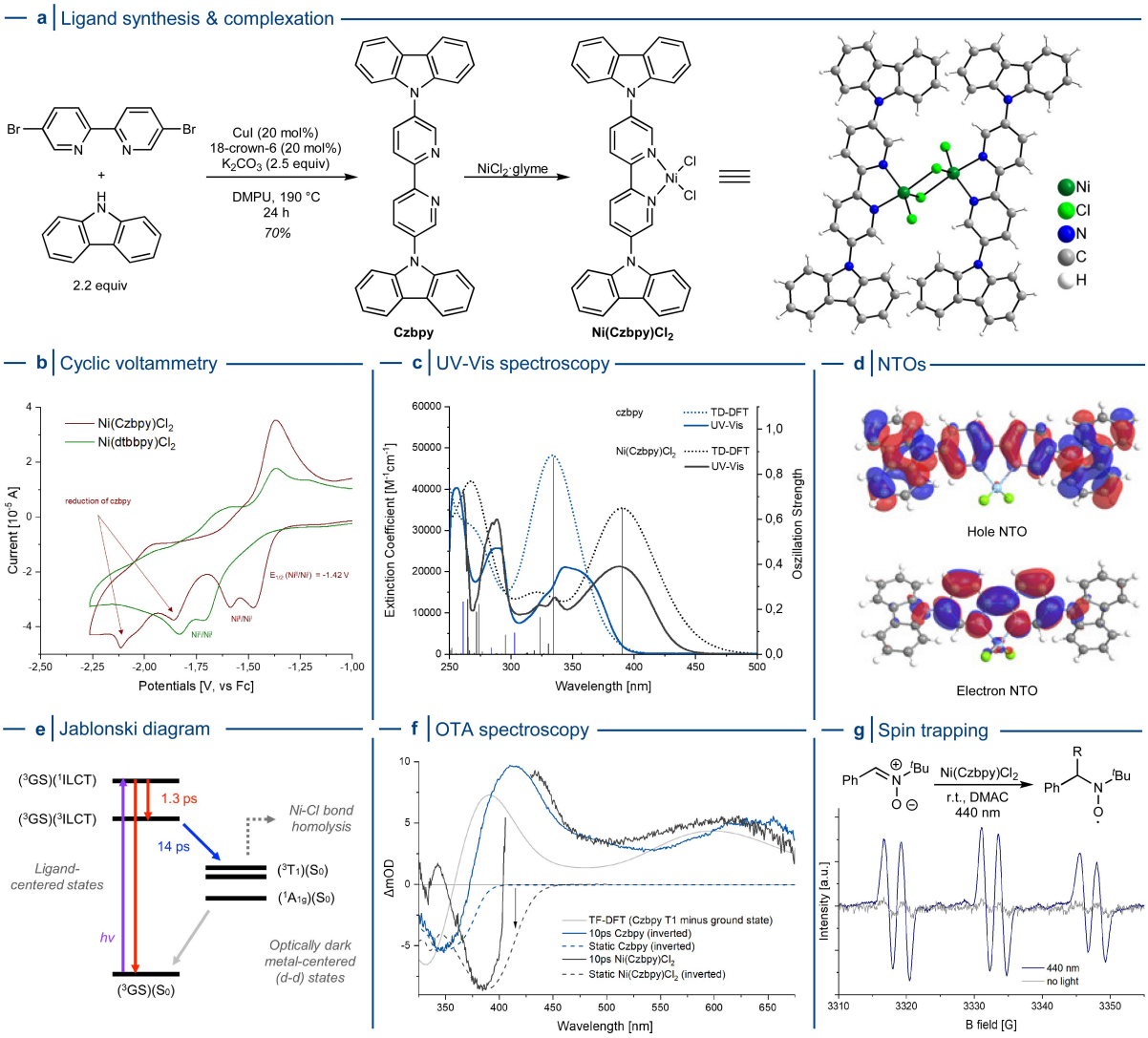

Figure 2. Synthesis and characterization of Czbpy and Ni(Czbpy)Cl_2. a) The ligand was synthesized via an Ullmann C–N coupling and forms the desired complex upon treatment with $NiCl_2$·glyme. b) Cyclic voltammetry studies of Ni(Czbpy)Cl_2 and Ni(dtbbpy)Cl_2. c) Experimental and calculated UV/Visible spectra of Czbpy and Ni(Czbpy)Cl_2. The band indicated by a vertical line is assigned to an intraligand charge transfer (ILCT) transition. The theoretical spectra have been shifted by −0.25 eV. d) Natural transition orbitals (NTOs) of Ni(Czbpy)Cl_2. e) A simplified excited state relaxation diagram of Ni(Czbpy)Cl_2. The states are separately labeled for the metal center and Czbpy ligand in parenthesis, respectively. f) Optical transient absorption data of Ni(Czbpy)Cl_2 and Czbpy at 10 ps after photoexcitation at 415 nm (arrow). For comparison, the inverted static absorption spectra are shown as well. The solid black curve is the simulated transient spectrum from TD-DFT calculated by subtracting the ground state spectrum from the spectrum of the lowest-triplet T1 state. The spectra have been arbitrarily scaled to approximately match the amplitude of the transient czpbpy spectrum (blue). g) Spin trapping experiment of Ni(Czbpy)Cl_2 in DMAc in the presence of phenyl *N*-*t*-butylnitrone (PBN) with and without illumination. Radical species are formed upon irradiation.

orbital is of Cz π character and the lowest unoccupied molecular orbital is of bpy π* character; Figure 2d, Figure S37, and Table S2). A similar transition was assigned to the 343 nm band of the unbound Czbpy ligand (Table S3). The red-shift of the ILCT band upon complexation is due to a slight delocalization of electron density involving Ni and Cl atoms.

We conducted femtosecond-resolved optical transient absorption (OTA) experiments to elucidate the excited-state relaxation pathway for this complex (see the Supporting Information for details). Upon excitation into the ILCT band at 415 nm, the complex undergoes a fast (~ ~1.3 ps) intersystem crossing from a singlet to a triplet ILCT state, convolved with a partial back relaxation to the ground state on the same time scale (Figure 2e). Within ~14 ps, the triplet ILCT decays into an optically dark excited state manifold. This assignment is supported by OTA experiments and TD-DFT on the bare ligand. Figure 2f compares the transient spectra of the Ni(Czbpy)Cl_2 complex and the Czbpy ligand at 10 ps after photoexcitation. The transient spectra of the complex and ligand are similar, except for an energy shift as expected from the ground-state spectra (Figure 2c). Furthermore, we simulated the transient spectrum of the ligand using TD-DFT; the difference between

the TD-DFT spectrum of the lowest ligand-centered triplet state (with ILCT character) and of the ground state matches the transient spectra strikingly well. These findings corroborate the finding that the ~14 ps excited state of Ni(Czbpy)Cl_2 corresponds to a triplet intraligand excited state with charge-transfer character.

While the ground state adopts a tetrahedral geometry and is of triplet character, the lowest lying excited d-d state is square-planar and of singlet $^1A_{1g}$ character (Figure S34). Several triplet d-d $^3T_1$ states are calculated to lie between the ILCT and singlet $^1A_{1g}$ states (Figure S38). We propose that the triplet ILCT state decays into this metal-centered d-d state manifold, while a partial back relaxation to the ground state on the same time scale may also occur. The excited d-d states are optically dark, meaning that they cannot be detected in the UV/Visible part of the spectrum. Indeed, the ground-state spectrum is dominated by ligand-centered absorption bands that are not expected to be different for the metal-centered states. The ^{1}(d-d) and ^{3}(d-d) states have anti-bonding character along the nickel halide bonds (Figure S39), signifying their propensity for Ni–Cl bond homolysis and the formation of catalytically active Ni^I species. A similar pathway has been suggested in other catalytic nickel complexes.[14,23] We note, however, that in similar Ni(bipyridine) aryl halide complexes, repulsive ligand-to-metal charge-transfer (LMCT) excited state potential energy surfaces were invoked in Ni-aryl bond homolysis.[16,17] While the involvement of such surfaces cannot be excluded here, the LMCT states are expected to lie much higher in energy in Ni dichloride complexes compared to Ni heteroaromatic complexes. A crossing from the relatively low-lying ILCT states onto such LMCT surfaces is thus unlikely in the present case.

Electron paramagnetic resonance (EPR) spin-trapping experiments clearly showed the formation of a spin adduct when a mixture of Ni(Czbpy)Cl_2 and phenyl *N*-*tert*-butylnitrone (PBN) is irradiated with 440 nm LEDs at room temperature (Figure 2g, see the Supporting Information for details). The spectrum resulting from illumination of Ni(Czbpy)Cl_2 and PBN in DMAc is characteristic for a spin adduct of an O- or C-centered radical rather than a chlorine radical. Chlorine radicals are difficult to identify using spin-trap methods, because trapping products are typically unstable.[24] More specifically, the resulting Ni^I complex potentially re-abstracts chlorine from the spin adduct to regenerate the Ni^{II} complex.[25] However, we assume that the chlorine radical reacts with DMAc to generate an O- or C-centered radical species that is responsible for the EPR signal in the trapping experiment using 440 nm irradiation.

Building on these favorable properties (strong absorption band in the visible and the formation of labile excited states and radical species), we investigated if in situ-formed Ni(Czbpy)Cl_2 serves as a suitable nickel precatalyst for carbon–heteroatom cross-couplings that mitigates the necessity of an exogenous photocatalyst for its activation (Figure 3).[26] The coupling of aryl halides with sodium sulfinate salts was originally reported using combinations of a nickel catalyst with iridium[27] or ruthenium[28,29] polypyridyl complexes as photocatalysts. Irradiating a mixture of 4-iodobenzotrifluoride, sodium 4-methylbenzenesulfinate, $NiCl_2$·glyme, and Czbpy in DMSO with 440 nm LEDs afforded sulfone **1** in excellent yield after 22 h (Figure 3a, entry 1). No conversion was detected when the reaction was carried out in the dark (entry 2). Sodium sulfinates and aryl halides can assemble in electron-donor acceptor (EDA) complexes and afford sulfones upon UV light irradiation.[30] Accordingly, even in absence of $NiCl_2$·glyme small amounts of **1** were formed due to partial emission in the UV region of the light source (entry 3). When 2,2′-bipyridine (bpy), 9*H*-carbazole or a combination of bpy and 9*H*-carbazole were used, the desired product was also formed, although with low selectivity (entries 4–6).

The C–O arylation of 4-iodobenzotrifluoride with *N*-Boc-proline under optimized conditions resulted in 88 % of the desired product (**2**) (Figure 3b, entry 7). No product formation was observed in the dark, without $NiCl_2$·glyme, or when 9*H*-carbazole was used as a ligand (entries 8–10). Only small amounts (<10 %) of **2** were formed using bpy, or bpy together with 9*H*-carbazole (entries 9, 11). This transformation was used to probe if the proposed Ni^I/Ni^{III} cycle could perpetuate if light irradiation is interrupted. We indeed observed a significant increase in product formation when the reaction was subjected to photon-free conditions after 6 h irradiation, supporting the overall mechanistic proposal (see the Supporting Information for details).

The light-mediated, nickel-catalyzed *N*-arylation of 4-methylbenzenesulfonamide afforded **3** in 75 % yield (Figure 3c, entry 13). Light and the nickel salt were crucial for product formation (entries 13, 14). Partial consumption of the starting material in the absence of a nickel salt (entry 15) might be a result of a photocatalytic activation of aryl iodides.[31] Product formation was not detected using bpy (entry 17), but significant amounts of **3** were obtained in the presence of 9*H*-carbazole (entry 16) or a combination of 9*H*-carbazole and bpy (entries 16 and 18). This might result from formation of a Ni-carbazole complex that induces cross-coupling reactions through MLCT.[32,33]

Czbpy was not suitable as a ligand for coupling of aryl halides with amines or thiols, and only low amounts of the respective coupling product was obtained when an alcohol was used as a nucleophile (Tables S27–S29).[6] Attempts to form carbon–carbon bonds through coupling of aryl halides with trifluoroborates[34] or α-silylamines[35] did not meet with success or suffered from low selectivity (Tables S30–S32).

The scope and limitations of photocatalyst-free, visible-light-mediated carbon–heteroatom cross-coupling reactions were explored next (Table 1). Aromatic sulfinate salts were coupled with 4-iodobenzotrifluoride (Table 1a, **1**, **4**–**7**). Optimized reaction conditions did not result in the desired product using sodium methane sulfinate. This substrate was earlier reported as a successful coupling partner when Ni(bpy)Cl_2 was used in combination with tris(2,2′-bipyridyl)-dichlororuthenium(II) hexahydrate as an exogenous photocatalyst.[29] With regard to the aryl iodide, the reaction affords the corresponding sulfones in the presence of electron-withdrawing groups such as trifluoromethyl (**1**), nitrile (**8**), ketone (**9**–**11**), amide (**12**), boron pinacolate ester (**13**), and methyl ester (**14**). *Para*- (**9**) and *ortho*- (**11**)

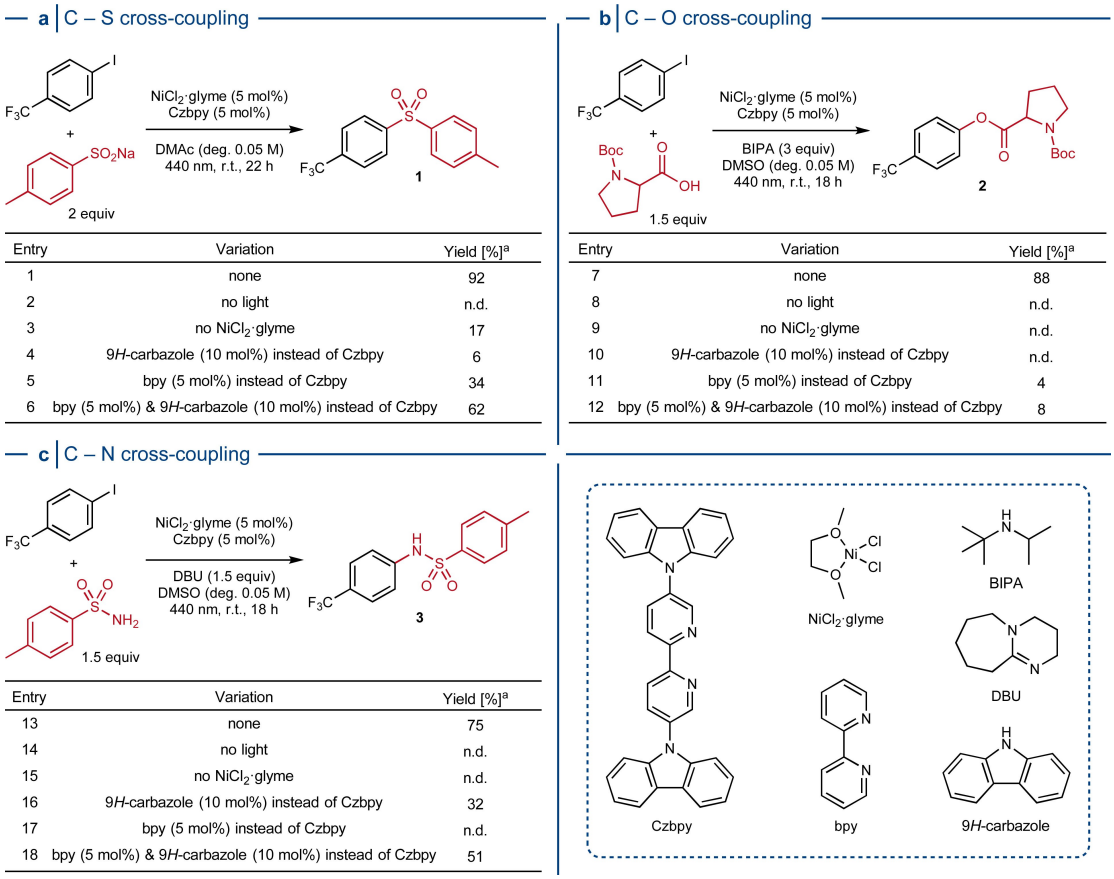

Entry	Variation	Yield [%][a]
1	none	92
2	no light	n.d.
3	no $NiCl_2$·glyme	17
4	9*H*-carbazole (10 mol%) instead of Czbpy	6
5	bpy (5 mol%) instead of Czbpy	34
6	bpy (5 mol%) & 9*H*-carbazole (10 mol%) instead of Czbpy	62

Entry	Variation	Yield [%][a]
7	none	88
8	no light	n.d.
9	no $NiCl_2$·glyme	n.d.
10	9*H*-carbazole (10 mol%) instead of Czbpy	n.d.
11	bpy (5 mol%) instead of Czbpy	4
12	bpy (5 mol%) & 9*H*-carbazole (10 mol%) instead of Czbpy	8

Entry	Variation	Yield [%][a]
13	none	75
14	no light	n.d.
15	no $NiCl_2$·glyme	n.d.
16	9*H*-carbazole (10 mol%) instead of Czbpy	32
17	bpy (5 mol%) instead of Czbpy	n.d.
18	bpy (5 mol%) & 9*H*-carbazole (10 mol%) instead of Czbpy	51

Figure 3. Optimized reaction conditions and control experiments for light-mediated carbon–heteroatom cross-coupling reactions catalyzed by Ni(Czbpy)Cl_2. a) C–S arylation of sodium *p*-toluensulfinate with 4-iodobenzotrifluoride. b) C–O arylation of *N*-Boc-proline with 4-iodobenzotrifluoride. c) C–N arylation of *p*-toluensulfonamide with 4-iodobenzotrifluoride. [a] NMR yields determined by ^{1}H NMR spectroscopy using 1,3,5-trimethoxybenzene as an internal standard. n.d. = not detected.

substitution showed similar reactivity, whereas *meta*-substitution (**10**) required longer reaction time. Electron-rich aryl iodides, such as 4-iodotoluene (**15**) and 4-iodoanisole (**16**), were suitable substrates and the presence of an unprotected amine group (**17**) was tolerated. Coupling of 2-iodothiophene (**18**) and 4-iodopyridine (**19**) showed that heteroaryl iodides are suitable substrates. Aryl iodides reacted significantly faster than the corresponding bromide (**14**). This is in contrast to dual nickel/photocatalytic protocols, where iodides and bromides exhibit similar reactivity.[27,28] Aryl chlorides undergo nickel/photocatalytic reactions when the more electron-donating ligand 4,4′-dimethoxy-bpy is used in combination with a exogenous photocatalyst,[27] but Czbpy was not suitable. These observations were applied for selective couplings of aryl iodides that contain a chloride (**20**) or a bromide substituent (**21**). Moreover, diarylated product **22** was synthesized from 1,4-diiodobenzene.

Good to excellent isolated yields were obtained for the C–O arylation of 4-iodobenzotrifluoride with aliphatic and aromatic carboxylic acids (Table 1b, **2**, **23**–**26**). A range of aryl iodides containing electron-withdrawing groups afforded the corresponding products (**2**, **27**–**35**). Longer reaction times were required for the coupling of *meta*-substituted aryl iodides (**27**, **29**, **31**), compared to their *para*-substituted analogues (**28**, **30**, **32**). The coupling of *ortho*-substituted aryl iodides was not possible in case of 2-iodoacetophenone and 2-iodobenzonitrile, but **36** was successfully synthesized from methyl 3-methyl-4-iodobenzoate. A heteroaryl iodide was also susceptible to the optimized reaction conditions (**38**). High electron densities on the aryl iodide decreased their reactivity towards the C–O coupling, as showcased for the series 4-iodobenzene (**38**), 4-iodotoluene (**39**), and 4-iodoanisole (**40**). Aryl iodides work best in the reaction (**32**, 90 % from Ar-I). The reaction is rather slow using the corresponding bromide (46 % NMR yield from Ar-Br), and a chloride afforded only traces of the desired product. As a result, 1-chloro-4-iodobenzene (**41**) coupled selectively on the iodo-position, but 1-bromo-4-iodobenzene reacted unselectively. These results are in agreement with previous reports on the dual nickel/photocatalytic cross-coupling.[13,31,36–38]

Aromatic and aliphatic sulfonamides (**3**, **42**–**46**) gave selective C–N cross-couplings with 4-iodobenzotrifluoride (Table 1c). In contrast to the C–S and C–O coupling, reactivity is not affected by the substitution pattern of the aryl iodide (**47**–**49**, **54**) or by the presence of either electron-withdrawing or -donating functional groups (**3**, **47**–**53**, **56**–**58**). Heteroaryl halides are problematic substrates in dual

Table 1: Visible-light-mediated nickel-catalyzed C–S, C–O and C–N cross-couplings.[a]

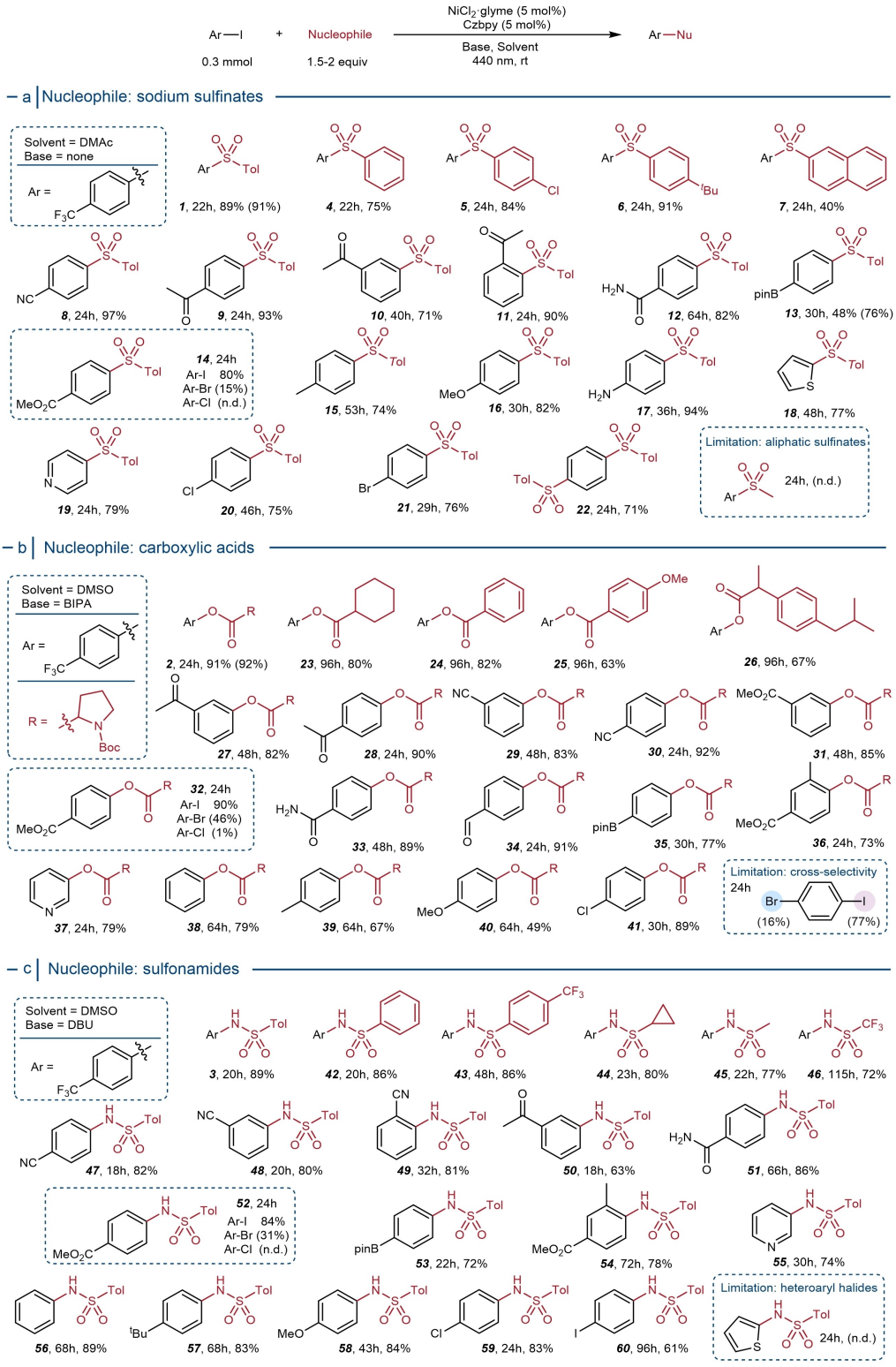

[a] Reaction conditions: aryl halide (300 μmol), nucleophile (panel a, sodium sulfinate, 600 μmol; panel b, carboxylic acid, 450 μmol; panel c, sulfonamide, 450 μmol), $NiCl_2$·glyme (15 μmol), Czbpy (15 μmol), base (panel b, *N-tert*-butylisopropylamine, 900 μmol; panel c, 1,8-diazabicyclo-[5.4.0]undec-7-ene, 450 μmol), solvent (panel a, DMAc, 6 mL; panel b, DMSO, 3 or 6 mL; panel c, DMSO, 6 mL), 440 nm LED (2 lamps at full power) at room temperature. Isolated yields are reported. NMR yields are in parentheses and were calculated via ^{1}H NMR spectroscopy using 1,3,5-trimethoxybenzene or maleic acid as an internal standard. n.d. = not detected. Bpin = boronic acid pinacolate ester. BIPA = *N-tert*-butylisopropylamine. DBU = 1,8-diazabicyclo[5.4.0]undec-7-ene.

nickel/photocatalytic sulfonamidation protocols and require a ligand-free approach at elevated temperature.[39] Under our optimized conditions 3-iodopyridine gave **55** in good yield, but no product was observed for 2-iodothipohene. Previously, aryl bromides were coupled with sulfonamides using combinations of nickel and iridium catalysts.[39] Aryl bromides are suitable substrates but iodide reactivity is superior (**52**, 84 % from Ar-I, 31 % NMR yield from Ar-Br within 24 h). Aryl chlorides are not reactive and **59** was obtained with good selectivity from 1-chloro-4-iodobenzene.

Having shown that Czbpy serves as a versatile ligand for visible-light-mediated cross-coupling reactions via homogeneous nickel catalysis, we aimed to extend this approach to develop a heterogeneous, recyclable catalyst.[40] Defined porous materials are ideal candidates for immobilization of metal catalysts, as they enable optimal access to the catalytic sites. The microporous organic polymer network poly-Czbpy was synthesized from Czbpy via oxidative polymerization and exhibits a Brunauer–Emmett–Teller surface area (S_{BET}) of 853 $m^2 g^{-1}$ (Figure 4a, see the Supporting Information for details).[22] The chemical structure of poly-Czbpy was confirmed by ^{13}C CPMAS NMR spectroscopy showing signals between 130 and 152 ppm (Figure S4), which verify the existence of bipyridine moieties within the structure. Additionally, at 137 ppm a signal corresponding to carbons in vicinity to carbazolyl nitrogen C_{Ar}-N was detected. Ni@poly-Czbpy was prepared by refluxing a suspension of poly-Czbpy and $NiCl_2$ in methanol. Investigation of the porosity showed a decreased BET surface of 470 $m^2 g^{-1}$ due to the immobilization of Ni^{II}. Presence of nickel shifts the absorption of the material up to 650 nm, while the metal-free ligand framework poly-Czbpy absorbs until 550 nm (Figure 4b). Characterization of Ni@poly-Czbpy by X-ray photoelectron spectroscopy (XPS) confirmed successful immobilization of Ni^{II} species on the polymeric material (Figure 4c). The N 1s core spectrum contains three signals for nitrogen: i) an intense peak at 400.4 eV corresponding to polymerized carbazole moieties, ii) a signal at 399.7 eV which is assigned to N–Ni coordination of the Ni^{II}-complex and iii) a low-intensity peak at 400.2 eV derived from bipyridine nitrogen species that are not coordinated to nickel. The Ni 2p spectrum shows a doublet and its corresponding satellites. Peaks located at 855.6 eV and 873.3 eV are assigned to Ni $2p_{3/2}$ and Ni $2p_{1/2}$ signals for Ni^{II} species, respectively. ICP-OES analysis indicated the presence of 3.7 % w/w of nickel, corresponding to an occupation of 40 % of bipyridine functionalities. Scanning electron microscopy (SEM) images of Ni@poly-Czbpy show the morphology of the amorphous polymeric particles (Figure S5). The images depict a homogeneous distribution of nickel, nitrogen, and chlorine within the material.

After confirming that poly-Czbpy is suitable to coordinate and immobilize nickel atoms, its use in the coupling reactions was studied (Figure 4d). The desired C–S, C–O, and C–N coupling products were obtained by irradiation at 440 nm of mixtures of $NiCl_2$·glyme (5 mol %) and poly-Czbpy (5 mol %), but the selectivity was initially lower than using homogeneous conditions. According to ICP-OES analysis, 40 % of the pyridine sites in poly-Czbpy coordinate to nickel. Therefore, equimolar amounts of nickel and poly-Czbpy lead to an excess of unligated nickel in solution that presumably has a detrimental effect on the selectivity. This was confirmed during a series of experiments using a lower nickel salt/macroligand ratio (2.5 mol % of $NiCl_2$·glyme, 5 mol % poly-Czbpy) that improved selectivity for all transformations significantly.

Next, we studied whether the heterogeneous catalytic system based on poly-Czbpy can be recycled. The heterogeneous material was recovered after the C–S coupling reaction by centrifugation and was reused for the same reaction (Figure 4e). Initial results confirmed that poly-Czbpy can be recycled ten times without significant loss in reactivity using 5 mol % $NiCl_2$·glyme for each reaction cycle (orange bars). The addition of the nickel salt at each reaction cycle was not necessary (green bars) and the selectivity of the reaction improved upon washing and reusing the material without addition of fresh nickel salt (1st cycle: 78 % yield, 2nd cycle: 90 % yield). This supported our earlier observation that an excess of unligated nickel results in lower selectivity. A final recycling experiment was carried out by adding 2.5 mol % of $NiCl_2$·glyme for the first reaction cycle (Figure 4e, blue bars) and resulted in excellent yields for the C–S coupling reaction without significant loss in activity during ten recycling experiments. The Ni 2p XPS spectra of the recycled catalyst confirmed that the Ni^{II} species remained intact within the polymer (Figure S53). The signals for the doublet were detected at 856.6 eV (Ni $2p_{3/2}$) and 874.6 eV (Ni $2p_{1/2}$), respectively. Furthermore, N 1s XPS core-level spectra show that, by single addition of Ni^{II} precursor, predominantly the pyridinic nitrogen signal at 399.2 eV was detected due to a relatively low amount of Ni^{II} coordinated to bipyridine, while addition of Ni^{II} after each cycle result mainly in Ni–N coordination signals at 399.7 eV (Figure S54).

The promising results of the recycling studies prompted us to study the long-term stability of the heterogeneous catalyst in a continuous flow packed-bed reactor.[41] Here, the heterogeneous catalyst remains located in a specific part of the reactor through which the reaction mixture is pumped. The desired chemical reaction and separation of the catalyst from the solution take place simultaneously, enabling straightforward studies on the robustness of the polymeric ligand and metal leaching.[42] We carried out a continuous long-run C–S cross-coupling experiment over seven days using a mixture of poly-Czbpy, silica and glass beads in an irradiated packed-bed reactor (Figure 4f, see the Supporting Information for details). To our delight, a stable catalytic activity was observed after reaching steady-state conditions and a total nickel leaching of only ~15 % was determined.

Conclusion

Installing two carbazole units on a bipyridine motif enables the formation of a homogeneous Ni^{II} complex that absorbs at up to 450 nm and enables visible-light-mediated C–S, C–O, and C–N cross-coupling reactions without the addition

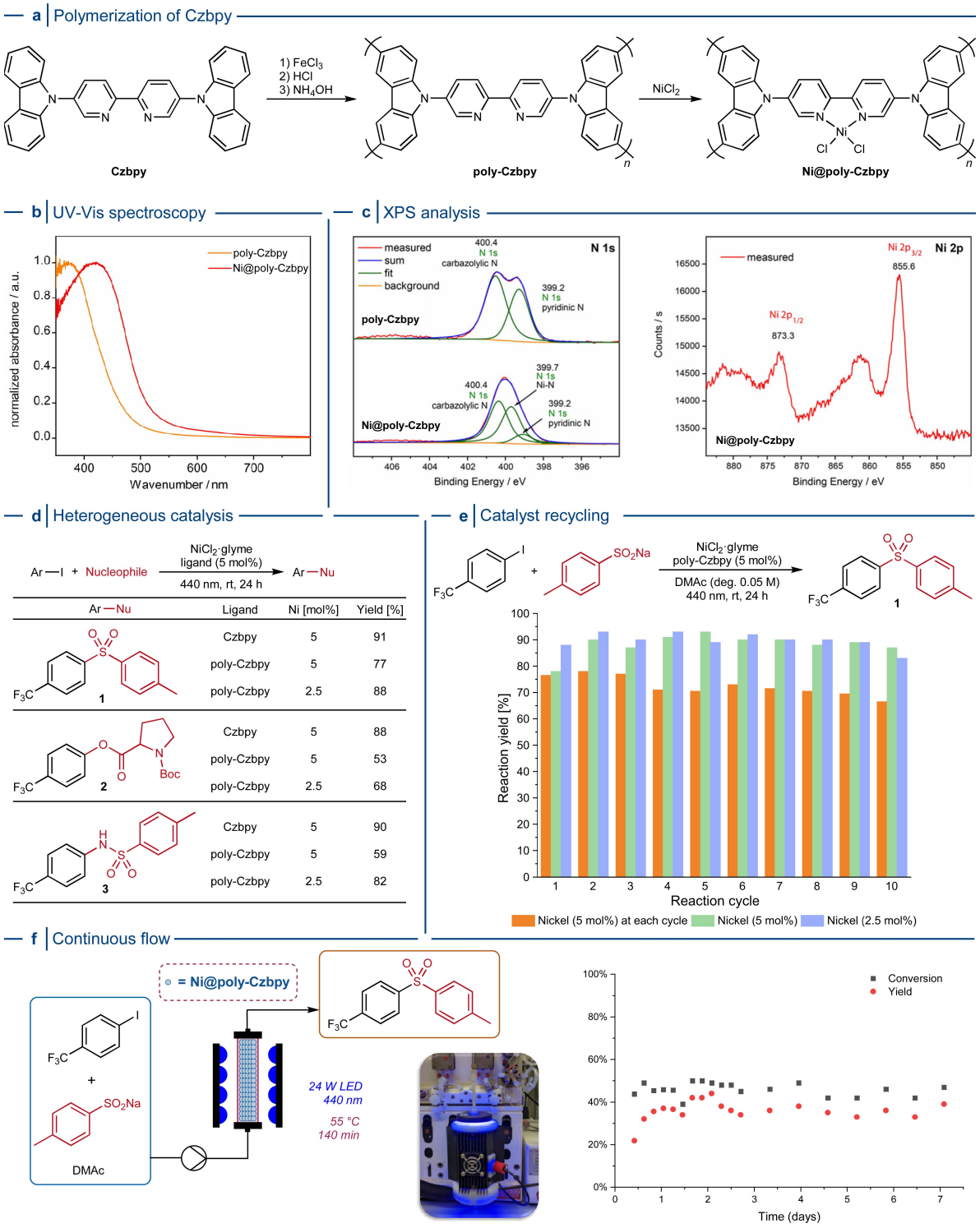

Ar—Nu	Ligand	Ni [mol%]	Yield [%]
1	Czbpy	5	91
	poly-Czbpy	5	77
	poly-Czbpy	2.5	88
2	Czbpy	5	88
	poly-Czbpy	5	53
	poly-Czbpy	2.5	68
3	Czbpy	5	90
	poly-Czbpy	5	59
	poly-Czbpy	2.5	82

Figure 4. Polymerization of Czbpy enables heterogeneous visible-light-mediated metallaphotocatalyzed cross-coupling reactions. a) Preparation of the porous organic polymer poly-Czbpy and complexation with $NiCl_2$. b) Characterization of poly-Czbpy and Ni@poly-Czbpy by UV/Visible spectroscopy. c) XPS analysis of Ni@Czbpy: N 1s and Ni 2p core-level spectra. d) Visible-light-mediated carbon–heteroatom cross-coupling reactions using Ni@poly-Czbpy as a heterogeneous metallaphotocatalyst. e) Catalyst recycling study (orange: 5 mol% of $NiCl_2$·glyme added at each reaction cycle; green: 5 mol% of $NiCl_2$·glyme added only for the first cycle; blue: 2.5 mol% of $NiCl_2$·glyme added only for the first cycle). f) Catalyst lifetime study using a continuous long-run C–S cross-coupling experiment over seven days flow in a packed-bed reactor.

of an exogenous photocatalyst. Studies using time-dependent density functional theory calculations, femtosecond-resolved optical transient absorption, and electron paramagnetic resonance spectroscopy revealed the formation of

a paramagnetic species upon irradiation of this complex with visible light, which occurs via a hitherto undisclosed initial intraligand charge transfer mechanism. This scenario holds significant potential for nickel catalysis and light-mediated (transition) metal catalysis in general, because it accesses light-responsive complexes solely through ligand excitation. Future work will focus on systematic variations of the Czbpy ligand scaffold to tune its electronic structure and correlate with photocatalytic reactivity, as well as multireference/multiconfigurational electronic structure calculations to investigate the potential role of higher-lying repulsive states and estimate the thermal barrier for Ni-chloride bond homolysis.[16,17]

In addition, the ligand scaffold can be easily converted into a porous organic polymer by a straightforward oxidative polymerization. The resulting macroligand immobilizes nickel for heterogeneous, visible-light-mediated nickel catalysis. The heterogeneous material recovered after the reaction can be reused, maintaining a high activity over ten reaction cycles. The robustness and reusability of the heterogeneous catalyst was further demonstrated during a flow experiment using a packed-bed reactor that showed stable conversion over seven days of continuous operation.

Acknowledgements

C.C., S.G., S.R., W.-H. H., N.R., L.A., D.C. P.H.S, and B.P. gratefully acknowledge the Max-Planck Society for generous financial support. S.G. and B.P. thank the International Max Planck Research School on Multiscale Bio-Systems for funding. B.P. acknowledges financial support by a Liebig Fellowship of the German Chemical Industry Fund (Fonds der Chemischen Industrie, FCI). H.M.-W., A.T,. and B.P. thank the Deutsche Forschungsgemeinschaft (DFG, German Research Foundation) under Germany's Excellence Strategy—EXC 2008-390540038—UniSysCat. S.V. and A.T. thank the Deutsche Forschungsgemeinschaft (DFG, German Research Foundation) for financial support (TH 1463/15-1). L.A. and B.P. thank the Deutsche Forschungsgemeinschaft (DFG, German Research Foundation) for financial support (BP 1635/2-19). R.M.V. acknowledges funding from the David and Lucile Packard Foundation. This material is based upon work supported by the U.S. Department of Energy, Office of Science, Office of Basic Energy Sciences under Award Number DE-SC0018904 to J.V.W. J.H.B. was supported by the Robert C. and Carolyn J. Springborn Endowment for Student Support Program and the National Science Foundation Graduate Research Fellowship Program. We thank Prof. R. Bittl and Dr. John J. Molloy for scientific support and fruitful discussions. Open Access funding enabled and organized by Projekt DEAL.

Conflict of Interest

The authors declare no conflict of interest.

Data Availability Statement

All experimental procedures and analytical data are available in the Supporting Information. All data is available from the authors on reasonable request.

Keywords: Flow Chemistry · Heterogeneous Catalysis · Homogeneous Catalysis · Photocatalysis · Nickel Catalysis

[1] A. Biffis, P. Centomo, A. Del Zotto, M. Zecca, *Chem. Rev.* **2018**, *118*, 2249–2295.
[2] P. Ruiz-Castillo, S. L. Buchwald, *Chem. Rev.* **2016**, *116*, 12564–12649.
[3] S. Z. Tasker, E. A. Standley, T. F. Jamison, *Nature* **2014**, *509*, 299–309.
[4] V. P. Ananikov, *ACS Catal.* **2015**, *5*, 1964–1971.
[5] J. Twilton, C. Le, P. Zhang, M. H. Shaw, R. W. Evans, D. W. C. MacMillan, *Nat. Chem. Rev.* **2017**, *1*, 0052.
[6] C. Zhu, H. Yue, J. Jia, M. Rueping, *Angew. Chem. Int. Ed.* **2021**, *60*, 17810–17831; *Angew. Chem.* **2021**, *133*, 17954–17975.
[7] C. Cavedon, P. H. Seeberger, B. Pieber, *Eur. J. Org. Chem.* **2019**, 1379–1392.
[8] A. Y. Chan, I. B. Perry, N. B. Bissonnette, B. F. Buksh, G. A. Edwards, L. I. Frye, O. L. Garry, M. N. Lavagnino, B. X. Li, Y. Liang, E. Mao, A. Millet, J. V. Oakley, N. L. Reed, H. A. Sakai, C. P. Seath, D. W. C. MacMillan, *Chem. Rev.* **2022**, *122*, 1485–1542.
[9] Z. H. Qi, J. Ma, *ACS Catal.* **2018**, *8*, 1456–1463.
[10] N. A. Till, L. Tian, Z. Dong, G. D. Scholes, D. W. C. MacMillan, *J. Am. Chem. Soc.* **2020**, *142*, 15830–15841.
[11] R. Sun, Y. Qin, S. Ruccolo, C. Schnedermann, C. Costentin, G. N. Daniel, *J. Am. Chem. Soc.* **2019**, *141*, 89–93.
[12] N. A. Till, S. Oh, D. W. C. MacMillan, M. J. Bird, *J. Am. Chem. Soc.* **2021**, *143*, 9332–9337.
[13] R. Sun, Y. Qin, D. G. Nocera, *Angew. Chem. Int. Ed.* **2020**, *59*, 9527–9533; *Angew. Chem.* **2020**, *132*, 9614–9620.
[14] S. I. Ting, S. Garakyaraghi, C. M. Taliaferro, B. J. Shields, G. D. Scholes, F. N. Castellano, A. G. Doyle, *J. Am. Chem. Soc.* **2020**, *142*, 5800–5810.
[15] B. J. Shields, B. Kudisch, G. D. Scholes, A. G. Doyle, *J. Am. Chem. Soc.* **2018**, *140*, 3035–3039.
[16] D. A. Cagan, D. Bím, B. Silva, N. P. Kazmierczak, B. J. McNicholas, R. G. Hadt, *J. Am. Chem. Soc.* **2022**, *144*, 6516–6531.
[17] D. A. Cagan, G. D. Stroscio, A. Q. Cusumano, R. G. Hadt, *J. Phys. Chem. A* **2020**, *124*, 9915–9922.
[18] G. Li, L. Yang, J. J. Liu, W. Zhang, R. Cao, C. Wang, Z. Zhang, J. Xiao, D. Xue, *Angew. Chem. Int. Ed.* **2021**, *60*, 5230–5234; *Angew. Chem.* **2021**, *133*, 5290–5294.
[19] L. Yang, H. H. Lu, C. H. Lai, G. Li, W. Zhang, R. Cao, F. Liu, C. Wang, J. Xiao, D. Xue, *Angew. Chem. Int. Ed.* **2020**, *59*, 12714–12719; *Angew. Chem.* **2020**, *132*, 12814–12819.
[20] T.-Y. Shang, L.-H. Lu, Z. Cao, Y. Liu, W.-M. He, B. Yu, *Chem. Commun.* **2019**, *55*, 5408–5419.
[21] T. Bortolato, S. Cuadros, G. Simionato, L. Dell'Amico, *Chem. Commun.* **2022**, *58*, 1263–1283.
[22] H. P. Liang, A. Acharjya, D. A. Anito, S. Vogl, T. X. Wang, A. Thomas, B. H. Han, *ACS Catal.* **2019**, *9*, 3959–3968.
[23] H. Na, L. M. Mirica, *Nat. Commun.* **2022**, *13*, 1313.
[24] A. Seto, Y. Ochi, H. Gotoh, K. Sakakibara, S. Hatazawa, K. Seki, N. Saito, Y. Mishima, *Anal. Methods* **2016**, *8*, 25–28.
[25] S. K. Kariofillis, A. G. Doyle, *Acc. Chem. Res.* **2021**, *54*, 988–1000.
[26] During the preparation of this manuscript, Li an co-workers developed a ligand that forms a complex with Ni^{II} salts, which

is also able to catalyze cross-couplings. This ligand also acts as a photocatalyst in absence of nickel. TD-DFT caluclations indicated that a MLCT transition is responsible for initiating cross-couplings: J. Li, C.-Y. Huang, C.-J. Li, *Chem* **2022**, *8*, 2419–2431.

[27] H. Yue, C. Zhu, M. Rueping, *Angew. Chem. Int. Ed.* **2018**, *57*, 1371–1375; *Angew. Chem.* **2018**, *130*, 1385–1389.

[28] M. J. Cabrera-Afonso, Z. P. Lu, C. B. Kelly, S. B. Lang, R. Dykstra, O. Gutierrez, G. A. Molander, *Chem. Sci.* **2018**, *9*, 3186–3191.

[29] N. W. Liu, K. Hofman, A. Herbert, G. Manolikakes, *Org. Lett.* **2018**, *20*, 760–763.

[30] L. Chen, J. Liang, Z. Y. Chen, J. Chen, M. Yan, X. J. Zhang, *Adv. Synth. Catal.* **2019**, *361*, 956–960.

[31] J. A. Malik, A. Madani, B. Pieber, P. H. Seeberger, *J. Am. Chem. Soc.* **2020**, *142*, 11042–11049.

[32] Y. S. Wong, M. C. Tang, M. Ng, V. W. Yam, *J. Am. Chem. Soc.* **2020**, *142*, 7638–7646.

[33] R. Alrefai, G. Hörner, H. Schubert, A. Berkefeld, *Organometallics* **2021**, *40*, 1163–1177.

[34] J. C. Tellis, D. N. Primer, G. A. Molander, *Science* **2014**, *345*, 433–436.

[35] C. Remeur, C. B. Kelly, N. R. Patel, G. A. Molander, *ACS Catal.* **2017**, *7*, 6065–6069.

[36] B. Pieber, J. A. Malik, C. Cavedon, S. Gisbertz, A. Savateev, D. Cruz, T. Heil, G. Zhang, P. H. Seeberger, *Angew. Chem. Int. Ed.* **2019**, *58*, 9575–9580; *Angew. Chem.* **2019**, *131*, 9676–9681.

[37] E. R. Welin, C. Le, D. M. Arias-Rotondo, J. K. McCusker, D. W. MacMillan, *Science* **2017**, *355*, 380–385.

[38] S. Reischauer, V. Strauss, B. Pieber, *ACS Catal.* **2020**, *10*, 13269–13274.

[39] T. Kim, S. J. McCarver, C. Lee, D. W. C. MacMillan, *Angew. Chem. Int. Ed.* **2018**, *57*, 3488–3492; *Angew. Chem.* **2018**, *130*, 3546–3550.

[40] S. Gisbertz, B. Pieber, *ChemPhotoChem* **2020**, *4*, 456–475.

[41] M. B. Plutschack, B. Pieber, K. Gilmore, P. H. Seeberger, *Chem. Rev.* **2017**, *117*, 11796–11893.

[42] R. Greco, W. Goessler, D. Cantillo, C. O. Kappe, *ACS Catal.* **2015**, *5*, 1303–1312.

Manuscript received: August 3, 2022
Accepted manuscript online: September 26, 2022
Version of record online: October 21, 2022